

# Structural and Magnetic Features of a FeCo-2V Alloy Processed by Metal Injection Molding

Borivoje Nedeljković, Nebojša Mitrović, *member IEEE*, Vladimir Pavlović

**Abstract**— In this paper the characterization of FeCo-2V alloys processed by metal injection molding (MIM) technology was investigated. The feedstock for MIM was prepared by mixing FeCoV powder with a low viscosity binder. Sintering of brown samples was performed during 3.5 hours from 1370 °C to 1460 °C in hydrogen atmosphere in order to attain the appropriate functional properties.

Microstructure and magnetic hysteresis B(H) of toroidal samples were investigated as a function of sintering temperature. An optimum magnetic properties were observed after sintering at temperature of 1370 °C. Magnetic properties were analyzed as frequency dependent in operating frequency range from 5 Hz to 60 Hz.

**Index Terms** — Metal injection moulding technology; FeCoV alloy, Structural properties, Magnetic properties

## I. INTRODUCTION

TECHNOLOGY of powder injection moulding (PIM) can offer very efficient manufacturing of ceramic or metallic parts with complex geometric shapes. Alloys that contain metal elements were produced by variation of PIM technology named metal injection molding (MIM) [1-3]. MIM as well as direct laser metal sintering (DLMS) process (where mixed metal powders are consolidated by laser in a single production step [4, 5]) are common and useful technologies for commercial production of many magnetic elements. Plenty of combinations of powders mixture, binders, molding techniques, debinding and sintering parameters, make MIM technology suitable for magnetic materials industry as it enables easier production of complex cores compared to the classical routes [6-8]. Unique magnetic properties can be obtained by mechanochemical processing of nanostructured Fe<sub>49</sub>Co<sub>49</sub>V<sub>2</sub> alloy [9, 10] as well as composite preparation [11].

Silva et. all [8] investigated equiatomic Fe50Co50 alloy produced by MIM without V addition and concluded that the elimination of vanadium can improve magnetic properties. It is possible to substantial decrease sintering temperature (980 °C instead of common sintering temperature of 1330 °C). Microstructure of the V containing alloy exhibits smaller grain size with increased porosity as a

main obstacles for magnetic domains movement resulting in the magnetic hardening. However, binary FeCo alloys are very brittle [12], and addition up to 2 % wt. of vanadium improves strength and ductility. Commercial functional material must poses both good mechanical and magnetic properties.

Advanced soft magnetic materials should exhibit a high saturation magnetic induction B<sub>S</sub> and relative magnetic permeability μ<sub>r</sub> as well as low core losses P<sub>core</sub> and coercive force H<sub>C</sub>. High Curie temperature T<sub>C</sub>, corrosion resistance and good mechanical properties are also very very important for some applications. Devices prepared from FeCo-2V alloy are usually exploited under extreme conditions (high operating temperature with high stress) and their functionality is associated with the unique combination of magnetic and mechanical properties. Iron-cobalt based alloys exhibit unique combination of high B<sub>S</sub> and T<sub>C</sub> as well as high corrosion resistance [12, 13]. The semi-hard magnetic alloy FeCo-2V is widely used in automation and electronics many of these parts are with complex shapes. Therefore, FeCoV alloy ferromagnetic parts for high temperature applications can be cost-effectively produced by MIM route.

## II. EXPERIMENTAL

In these experiments the feedstock was prepared by mixing the starting very fine powder and binder system that is easily removable by solvent and thermal debinding.

The investigated toroidal samples were produced by a Battenfeld HM 600/130 hydraulic drive injection moulding machine. A green cylindrical component with a central hole has 10 mm internal diameter, 18 mm external diameter and 28 mm length.

The injected green samples were first subjected to solvent debinding and subsequent thermal debinding followed by sintering with a holding time of 3.5 hours. The applied sintering procedure and atmosphere were taken from the classical procedure with pressed samples with a small modification of the initial stage of sintering to include thermal debinding. Secondary thermal debinding at optimized temperatures (up to 800 °C) and sintering in the temperature range 1370 °C - 1460 °C were performed on brown samples in a hydrogen atmosphere.

After this initial preparation the obtained samples had internal diameter of 8.5 mm and external diameter of 16 mm. Samples about 7.5 mm high were cut from the center section of the sintered piece, in order to achieve better measurement accuracy. Magnetic properties on toroidal core samples were measured at room temperature by Brockhaus Tester MPG 100 D that is common used for examination of

Borivoje Nedeljković – University of Kragujevac, Faculty of Technical Sciences in Čačak, Svetog Save 65, Serbia (e-mail: borivoje.nedeljkovic@ftn.kg.ac.rs)

Nebojša Mitrović – University of Kragujevac, Faculty of Technical Sciences in Čačak, Svetog Save 65, Serbia (e-mail: nebojsa.mitrovic@ftn.kg.ac.rs)

Vladimir Pavlović – Institute of Technical Sciences of SASA, Knez Mihailova 35/IV, Belgrade, (e-mail: vladimir.pavlovic@itn.sanu.ac.rs)

soft magnetic materials. The main properties such as coercive force  $H_C$ , saturation induction  $B_S$  and remanent induction  $B_r$  were determined from B-H loops. Maximum excitation was  $H_{max}=6$  kA/m at driving frequency set from 5 Hz to 60 Hz.

X-ray diffractograms of the samples after sintering were obtained using a Philips PW 1050 with  $Cu_{K\alpha}$  radiation ( $\lambda=0.154$  nm) and a step/time scan mode of  $0.05^\circ/1$  s. Scanning electron microscopy (SEM) JEOL JSM-6390 LV was used for microstructural characterization of the investigated samples after sintering process.

### III. RESULTS AND DISCUSSION

XRD diffraction patterns of FeCo-2V alloy samples sintered from  $1370^\circ\text{C}$  to  $1460^\circ\text{C}$  in hydrogen atmosphere are presented in Fig. 1. The clear evidence of the  $\alpha$ -FeCo crystalline phase by main diffraction peak around  $2\theta = 45^\circ$  is found for all investigated samples. An increase of sintering temperature is also followed by more intensive diffraction peaks that is especially evidenced on patterns 1.c and 1.d for samples sintered at  $1430^\circ\text{C}$  and  $1460^\circ\text{C}$ , respectively.

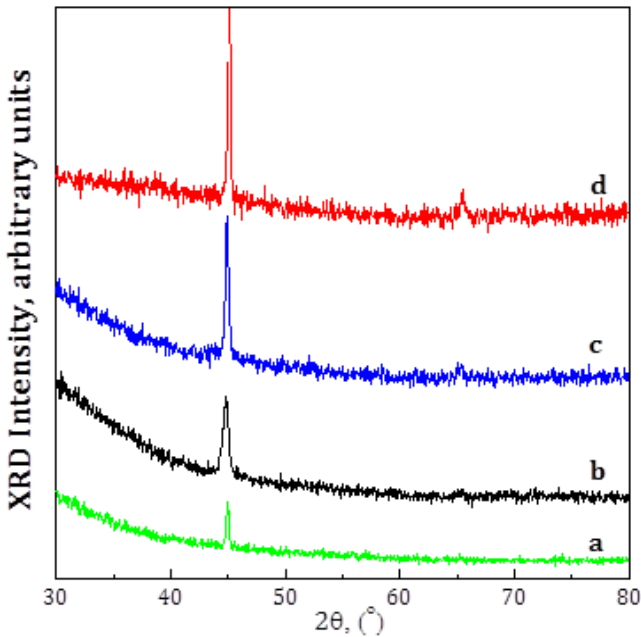


Fig. 1. XRD diffractograms of FeCo-2V alloy samples sintered with a holding time of 3.5 hours at temperature a)  $1370^\circ\text{C}$  b)  $1400^\circ\text{C}$ , c)  $1430^\circ\text{C}$  and d)  $1460^\circ\text{C}$  in hydrogen atmosphere.

Fig. 2. presents the iron  $\alpha$ -Fe (A2), cobalt  $\epsilon$ -Co (A3) and  $\alpha'$ -FeCo (B2) crystal phases, with appropriate magnetic features [14]. Evolved  $\alpha'$ -FeCo (B2) crystal phase is characterized by extremely high Curie temperature ( $T_c = 1390$  K that is even a little bit higher than the pure cobalt). Therefore, FeCo alloys with this crystal phase poses unique property of ferromagnetic behavior at high exploiting temperatures. Further, it can be observed increase in magnetic moment for both atoms ( $\alpha$ -Fe iron  $\mu_{Fe} = 2.218$   $\mu_B/\text{atom}$   $\rightarrow$   $\alpha'$ -FeCo  $\mu_{Fe} = 3.0$   $\mu_B/\text{atom}$ ,  $\epsilon$ -Co cobalt  $\mu_{Co} = 1.716$   $\mu_B/\text{atom}$   $\rightarrow$   $\alpha'$ -FeCo  $\mu_{Co} = 1.8$   $\mu_B/\text{atom}$ ), which

results in very high value of magnetic induction saturation  $B_S$  over 2 T.

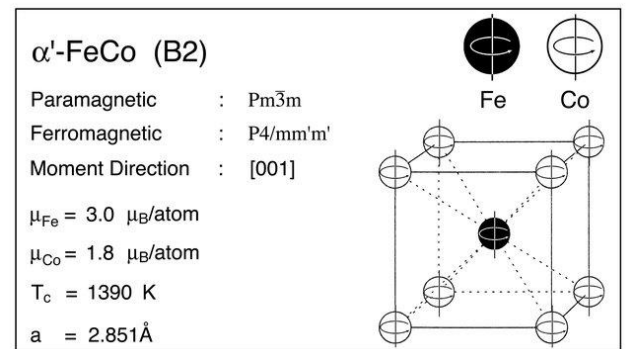
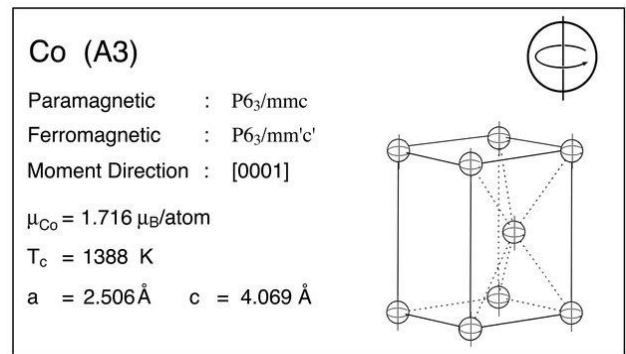
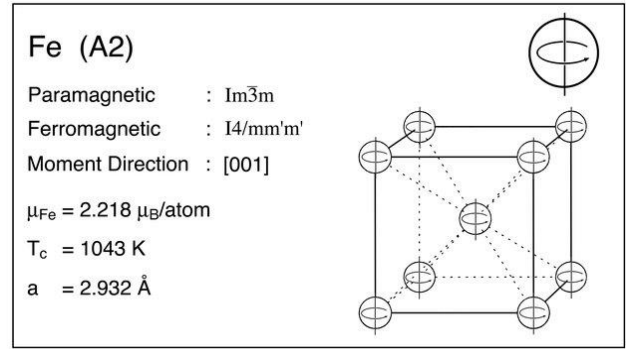


Fig. 2. Crystal structures for iron  $\alpha$ -Fe (A2), cobalt  $\epsilon$ -Co (A3) and  $\alpha'$ -FeCo (B2) phases, with magnetic features [14].

The SEM micrographs obtained from the surface of the investigated sintered samples are shown in Fig. 3. It can be seen that the powder particles were melted proportionally to the sintering temperature in the range from  $1370^\circ\text{C}$  to  $1460^\circ\text{C}$  (Figs. 3.a, 3.b, 3.c and 3.d).

The picture of the sample sintered at the highest temperature  $1460^\circ\text{C}$  unequivocally shows that the particles were completely melted. This is in good correlation with XRD pattern in Fig 1.d which exhibits the most intensive crystallization.

Fig. 4. shows the B(H) hysteresis loops broadening for minor curves ( $H_{max} = 6$  kA/m) for FeCo-2V sample sintered at  $1370^\circ\text{C}$  obtained at frequencies of 5 Hz, 10 Hz, 20 Hz, 40 Hz, 50 Hz and 60 Hz. It is well known that an increase in frequency leads to an increase in core power losses  $P_{tot}$  due to hysteresis losses  $P_h$ , normal eddy current losses as well as anomalous eddy current losses, respectively:  $P_{tot} = P_h + P_e + P_{an}$ .

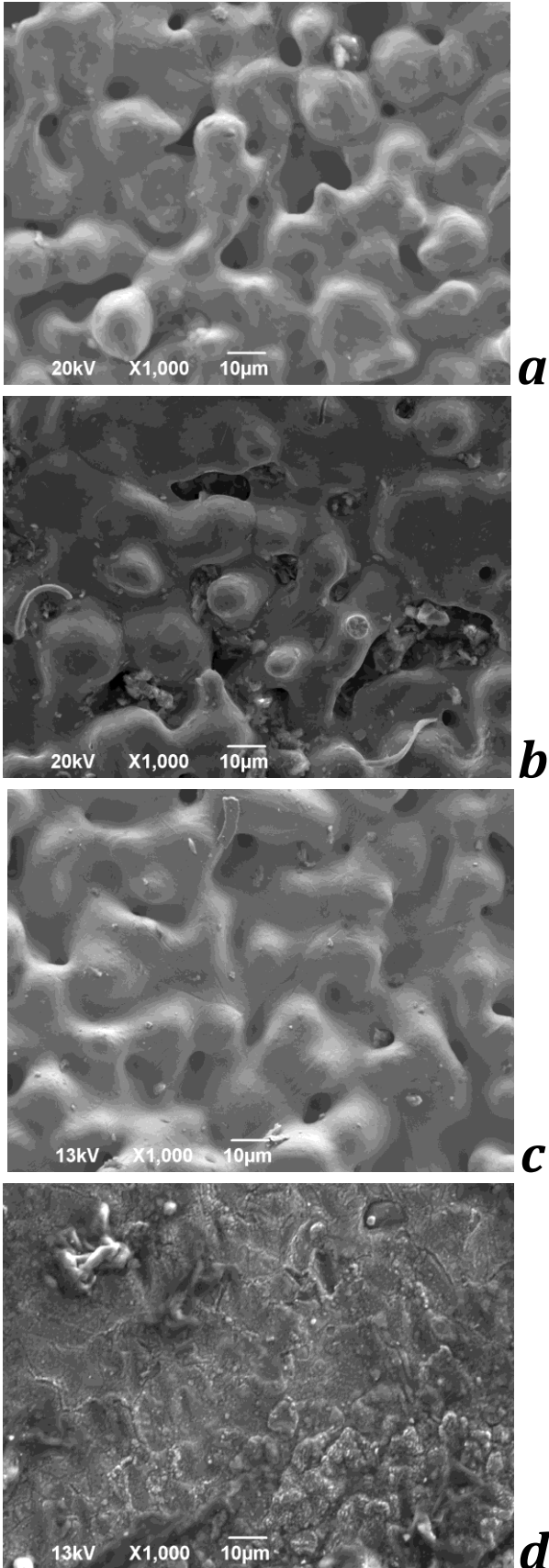


Fig. 3. Microstructures of FeCo-2V alloy samples sintered with a holding time of 3.5 hours at temperature a) 1370 °C b) 1400 °C, c) 1430 °C and d) 1460 °C in hydrogen atmosphere.

Fig. 5. shows the B(H) hysteresis loops broadening for FeCo-2V sample sintered at 1400 °C obtained at frequencies of 5 Hz, 10 Hz, 20 Hz, 40 Hz, 50 Hz ( $H_{max} = 6$  kA/m), as well as anomalous shape of dynamic loop at 60 Hz.

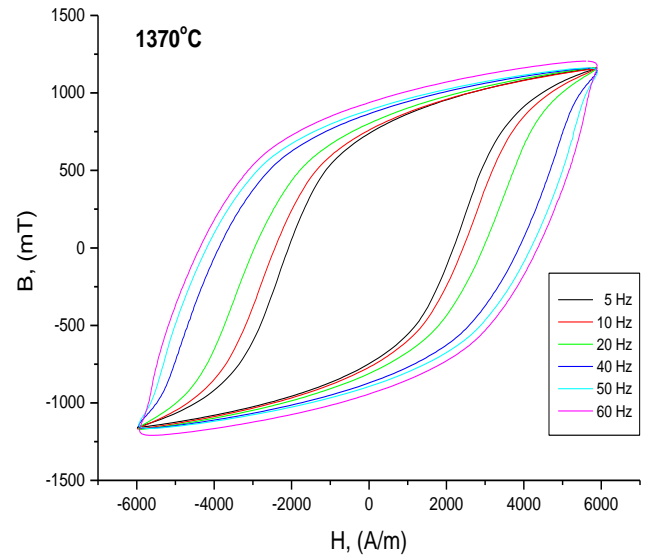


Fig. 4. The B(H) hysteresis loops broadening for FeCo-2V sample sintered at 1370 °C obtained at frequencies of 5 Hz, 10 Hz, 20 Hz, 40 Hz, 50 Hz and 60 Hz ( $H_{max} = 6$  kA/m).

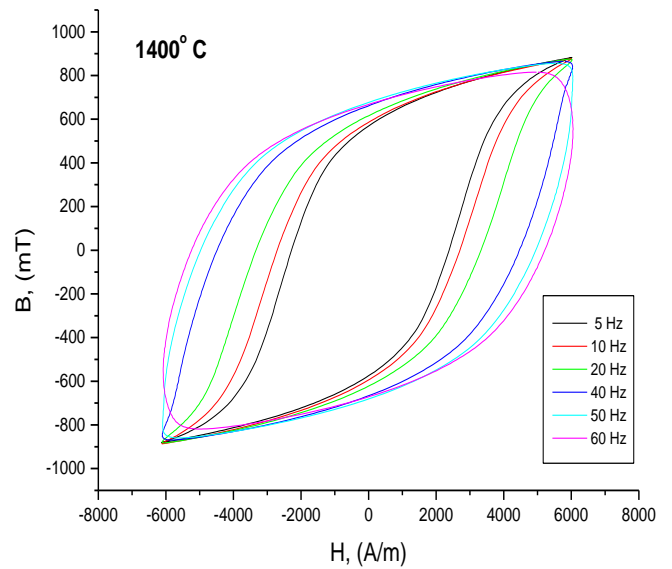


Fig. 5. The B(H) hysteresis loops broadening for FeCo-2V sample sintered at 1400 °C obtained at frequencies of 5 Hz, 10 Hz, 20 Hz, 40 Hz, 50 Hz and 60 Hz ( $H_{max} = 6$  kA/m).

It is performed numerical analysis of corective force on frequency  $H_C(f)$ , with the model already proposed by Grössinger et al [15]:

$$H_C(f) = a + b \cdot f^{1/2} + c \cdot f \quad (1)$$

where coefficient  $a$  correspond to the zero frequency coercivity that is extrapolated from the low frequency numerical data. The next two coefficients  $b$  and  $c$  describes the normal eddy currents and anomalous eddy currents, respectively.

The results of numerical analysis of corective force on frequency for samples sintered at 1370 °C and 1400 °C are presented on Fig. 6. (numerical data from the hysteresis lops obtained at frequencies of 5 Hz, 10 Hz, 20 Hz, 40 Hz, 50 Hz and 60 Hz ( $H_m = 6$  kA/m) presented on Fig. 4 and Fig. 5).

## ACKNOWLEDGMENT

This study was supported by the Ministry of Education, Science and Technological Development of the Republic of Serbia, and these results are parts of the Grant No. 451-03-68/2020-14/200132 with University of Kragujevac - Faculty of Technical Sciences Čačak.

## REFERENCES

- [1] H. Ye, X. Y. Liu, H. Hong, "Fabrication of metal matrix composites by metal injection molding-A review", *Journal of Materials Processing Technology*, 200 (2008) 12–24.
- [2] P. Setasuwon, A. Bunchavimonchet, S. Danchaivijit, "The effects of binder components in wax/oil systems for metal injection molding", *Journal of Materials Processing Technology*, 196 (2008) 94–100.
- [3] H. Shokrollahi, K. Janghorban, "Soft magnetic composite materials (SMCs)", *Journal of Materials Processing Technology*, 189 (2007) 1–12.
- [4] A. Simchi, "Direct laser sintering of metal powders: Mechanism, kinetics and microstructural features", *Materials Science and Engineering: A*, 428 (2006) 148–158.
- [5] Z. Ebersold, N. Mitrović, S. Đukić, B. Jordović, A. Peulić, "Defectoscopy of direct laser sintered metals by low transmission ultrasonic frequencies", *Science of Sintering*, 44 (2012) 177-185.
- [6] A. Silva, J. A. Lozano, R. Machado, J. A. Escobar, P. A. P. Wendhausen, "Study of soft magnetic iron cobalt based alloys processed by powder injection molding", *Journal of Magnetism and Magnetic Materials*, 320 (2008) e393–e396.
- [7] B. Zlatkov, N. Mitrović, M. V. Nikolić, A. Maričić, H. Danning, O. Aleksić, E. Halwax, "Properties of MnZn ferrites prepared by powder injection molding technology", *Materials Science and Engineering B-Advanced Functional Solid-state Materials*, 175 (2010) 217-222
- [8] A. Silva, J. A. Lozano, R. Machado, J. A. Escobar, P. A. P. Wendhausen, "Study of soft magnetic iron cobalt based alloys processed by powder injection molding", *Journal of Magnetism and Magnetic Materials*, 320 (2008) e393–e396.
- [9] A. Behvandi, H. Shokrollahi, B. Chitsazan, M. Ghaffari, "Magnetic and structural studies of mechanically alloyed nano-structured Fe<sub>49</sub>Co<sub>49</sub>V<sub>2</sub> powders", *Journal of Magnetism and Magnetic Materials*, 322 (2010) 3932–3937.
- [10] B. Chitsazan, H. Shokrollahi, A. Behvandi, O. Mirzaee, "Characterization and magnetic coercivity of nanostructured (Fe<sub>50</sub>Co<sub>50</sub>)<sub>100-x</sub>V<sub>x=0,2,4</sub> powders containing a small amount of Co<sub>3</sub>V intermetallic obtained by mechanical alloying", *Powder Technology*, 214 (2011) 105–110.
- [11] B. Weidenfeller, M. Anhalt, W. Riehemann, "Variation of magnetic properties of composites filled with soft magnetic FeCoV particles by particle alignment in a magnetic field", *Journal of Magnetism and Magnetic Materials*, 320 (2008) e362–e365.
- [12] T. Sourmail, "Near equiatomic FeCo alloys: Constitution, mechanical and magnetic properties", *Progress in Materials Science*, 50 (2005) 816–880.
- [13] G. B. Chon, K. Shinoda, S. Suzuki and B. Jeyadevan, "Order-disorder transformation in Fe<sub>50</sub>Co<sub>50</sub> particles synthesized by polyol process", *Materials Transactions*, 51 (2010) 707-711.
- [14] D. E. Laughlin, M. A. Willard, and M. E. McHenry, "Magnetic Ordering: Some Structural Aspects", Vol: Phase Transformations and Evolution in Materials, TMS Annual Meeting Conference, January 2000. Nashville, Tennessee.
- [15] R. Grössinger, N. Mehboob, D. Suess, R. Sato Turtelli, and M. Kriegisch, "An eddy-current model describing the frequency dependence of the coercivity of polycrystalline galfenol", *IEEE Transactions on Magnetics*, 48, pp. 3076-3079, 2012.

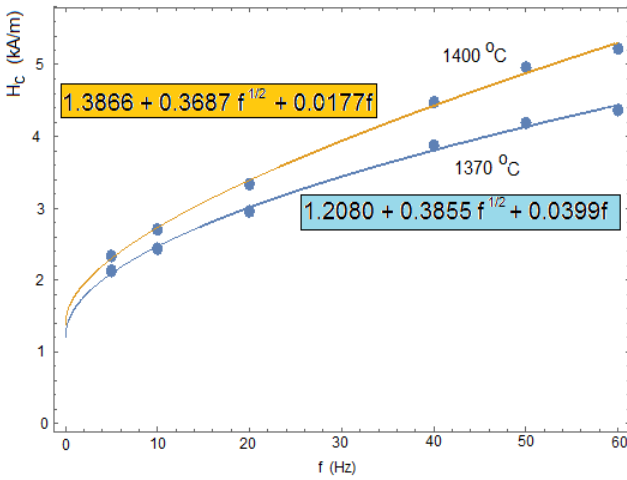


Fig.6. Dependence of coercivity on frequency  $H_c(f)$ , for FeCo-2V samples sintered at 1370 °C and 1400 °C.

Table I shows the analysis of the anomalous eddy currents at the frequencies of 5 Hz and 50 Hz for samples sintered at 1370 °C and 1400 °C. One can see for sample sintered at 1370 °C at low frequency of 5 Hz anomalous eddy currents influence  $H_{Cm}(f) = c \cdot f$  is only about 1 % and at high frequency of 50 Hz that influence is about 5 %. For sample sintered at 1400 °C at low frequency of 5 Hz anomalous eddy currents influence is 3.9 %, and at high frequency of 50 Hz that influence is high, i.e. about 18 %. Remanences for both hysteresis loops are similar: 0.77 for 1370 °C and 0.79 for 1400 °C.

Table I.

Zero frequency coercivity  $H_{c0}$ , total coercivity  $H_c$ , remanence ratio  $B_r/B_s$  and anomalous eddy currents influence at the frequencies of 5 Hz and 50 Hz for samples sintered at 1370 °C and 1400 °C.

	$a \cong H_{c0}$ (kA/m)	$H_c$ (kA/m)	$B_r/B_s$	$H_{Cm}(f)/$ $H_c(f)$
1370 °C	1,208	2,091 (5 Hz)	0.767	1 % (5 Hz)
1400 °C	1,387	2,299 (5 Hz)	0.792	3.9 % (5 Hz)
1370 °C	1,208	4,133 (50 Hz)	0.767	5 % (50 Hz)
1400 °C	1,387	4,880 (50 Hz)	0.792	18 % (50 Hz)

## IV. CONCLUSION

Characterization of near-equiatomic FeCo-based alloy with addition of 2 wt. % vanadium produced by MIM technology was performed. Only  $\alpha$ -FeCo crystalline phase is found for all investigated FeCo-2V alloy samples sintered from 1370 °C to 1460 °C in hydrogen atmosphere with a holding time of 3.5 hours. Powder particles sintered at the highest temperature 1460 °C were completely melted.

Magnetic measurements were performed in the operating frequency range from 5 Hz to 60 Hz with observed optimum magnetic properties for sample sintered at 1370 °C.

At high frequency of 50 Hz it is observed anomalous eddy currents influence of only about 5 % (sample sintered at 1370 °C), but for sample sintered at 1400 °C that influence is very high, about 18 %.